JTTEE5 19:756–764
DOI: 10.1007/s11666-010-9468-1
1059-9630/$19.00 © ASM International

Peer Reviewed

Process Design and Monitoring for Plasma Sprayed Abradable Coatings

Tanja Steinke, Georg Mauer, Robert Vaßen, Detlev Stöver, Dan Roth-Fagaraseanu, and Matthew Hancock

(Submitted July 17, 2009; in revised form September 16, 2009)

Abradable coatings in compressor and high-pressure stages of gas turbines must provide specific hardness and porosity values to achieve an optimal cut-in of the blade tips. A fractional factorial experimental plan was designed to investigate the influence of the plasma spraying parameters argon flow rate, current, spraying distance and powder feed rate on these properties of magnesia spinel. Based on the results, magnesia spinel coatings with low (~400 $HV_{0.5}$), medium (~600 $HV_{0.5}$) and high hardness (~800 $HV_{0.5}$) could be reliably manufactured. Further incursion rig tests confirmed the dependence of the rub-in behavior and abradability on the coating characteristics and process parameters, respectively. Process monitoring was also applied during plasma spraying of magnesia spinel abradables on batches of turbine components. The recorded particle characteristics and coating properties showed a good reproducibility of the spraying process.

Keywords coatings for engine components, coatings for gas turbine components, influence of spray parameters, porosity of coatings, PS microstructures, TBC topcoats

1. Introduction

Abradable coatings have been used in the compressor and high-pressure turbine stages of aerospace engines since the late 1960s. They are also becoming interesting for application in industrial gas turbines. They are applied to help minimize the clearance distance between the rotating blade tip and the stationary components that reduce tip leakage, leading to increases in efficiency and reductions in fuel consumption (Ref 1-5).

Abradable coatings are difficult to engineer because they have to be both abradable as well as mechanically stable at the same time to withstand the harsh operating conditions of a gas turbine. Typically, materials with porous, friable microstructures and therefore low shear strength are required. On low-pressure turbine stages with moderate temperatures both ceramic and metallic coatings have been used, while for high-pressure turbine applications mainly zirconia-based high-temperature abradables are used (Ref 2).

For applications at moderate temperatures in the compressor section of gas turbines, composite materials composed of a metal phase, a self-lubricating non-metal phase and a polymer for porosity generation (e.g. AlSi-polymer, AlSi-hBN, Ni-graphite and CoNiCrAlY-BN-polymer) are common materials. Their application depends also on the rubbing blade tip material as well as on the service temperatures (Ref 1).

For such composite materials with different physical properties of the individual components, it is very difficult to have good reliability in manufacturing them. Coatings often show homogeneity problems such that further developments have led to the investigation of full ceramic abradable coatings (Ref 4, 6).

A typical ceramic material which was investigated for application as a turbine abradable coating is yttria stabilized zirconia (YSZ). For moderate temperature applications, YSZ is used as a composite material with addition of organics and a solid lubricant (Ref 3), but for applications in the high-temperature field it is used as full ceramic coating (Ref 2). The limited temperature capability of about 1200 °C in long-term applications and the elevated surface temperatures due to the low thermal conductivity for thick abradable coatings are restricting factors for this material (Ref 7, 8).

Recently, new full ceramic materials of magnesia spinel structure have been developed to fulfill the requirements of abradability as well as resistance to high thermo-mechanical loading even at enhanced service temperatures above 1300 °C (Ref 9).

A convenient method for the application of abradable coatings is plasma spraying, where powder particles are injected into a plasma jet, becoming molten and accelerated, impact on a substrate and form the coating. The process can be carried out in atmosphere, inert gas or vacuum (Ref 10). The deposited particles (splats) are separated from each other by interlamellar pores resulting from rapid solidification, very fine voids formed by incomplete intersplat contact or around unmolten particles, and cracks due to thermal stresses (Ref 11). Such pores, voids and cracks represent the total porosity of the coating.

Tanja Steinke, Georg Mauer, Robert Vaßen, and **Detlev Stöver**, Forschungszentrum Jülich GmbH, Institut für Energieforschung IEF-1, 52425 Jülich, Germany; **Dan Roth-Fagaraseanu**, Rolls-Royce Deutschland Ltd & Co KG, Dahlewitz, Germany; and **Matthew Hancock**, Rolls-Royce plc, Derby, UK. Contact e-mail: t.steinke@fz-juelich.de.

During plasma spraying there are many influencing process parameters, e.g. current, plasma gas flow rates, powder size distribution, powder injection and feed rate are just a few examples. Usually several parameters are significant and can show interactions or opposite effects on specific coating properties (Ref 10). By creation of a process window the different parameters can be controlled to achieve the desired coating microstructures (Ref 12). For atmospheric plasma sprayed (APS) ceramic abradable coatings, hardness and porosity are important coating properties which need to be controlled reliably to achieve an optimal cut-in of the turbine blade tip without causing damage and material transfer of the blade (increase of unsealed gap).

A common way to set up a meaningful experimental investigation to describe such interdependencies is to use statistical methods based on the significance analysis of process parameters. In the simplest case, the potential parameters are each fixed at a low (−1) and a high (+1) level, whereby the experimental space is defined inside this parameter range (Ref 13).

The aim of this paper is to investigate the influence of plasma spraying parameters on the coating properties of APS sprayed non-stoichiometric magnesia spinel coatings. Because of the designated application as an abradable coating, the main focus in this work was laid on the target properties hardness and porosity. The deposition efficiency was also taken into account to achieve preferably cost-effective coating processes. For this investigation, a fractional factorial design of experiment (DoE) was used. The definition of a process window for magnesia spinel abradable coatings and the determination of suitable parameters to engineer a soft, medium and hard abradable coating were important issues. Furthermore, several investigations were performed to establish the best functional and quality test methods for this type of abradable coatings.

Table 1 Fractional factorial experimental plan

Run	Argon	Current	Spraying distance	Disc speed
1	−1	−1	−1	−1
2	−1	−1	1	1
3	−1	1	−1	1
4	−1	1	1	−1
5	1	−1	−1	1
6	1	−1	1	−1
7	1	1	−1	−1
8	1	1	1	1

2. Experimental

2.1 Setup of the DoE

To identify the significant spraying parameters and to analyze their impact on the coating characteristics, a fractional factorial experimental setup was chosen as given in Table 1. The four factors argon flow rate, current, spraying distance and disc speed of the powder feeder (corresponding to the powder feed rate) were each set to a low (−1) and a high (+1) level.

From this experimental setup $2^{(4-1)}$ coating runs result. Additionally, an interjacent standard parameter set (center point of the parameter space) was sprayed as reference. All coating runs are given in Table 2. The runs No. 0 and No. 9 correspond to the reference standard parameters.

2.2 Coating Preparation by Atmospheric Plasma Spraying

The coatings analyzed in this work were sprayed on a Sulzer Metco Multicoat facility (Sulzer Metco, Wohlen, Switzerland) with a F4 plasma torch mounted on a six-axis robot. The feedstock was a Jülich in-house produced non-stoichiometric, spray-dried alumina magnesia spinel powder AMO 278 I ($Mg_{1-x}Al_{2+x}O_4$). Figure 1 shows the SEM images of powder particles, and some characteristic data are given in Table 3.

The coatings were sprayed on grid-blasted 50 × 50 mm^2 mild steel substrates. Spraying parameters kept constant were the hydrogen flow rate, the robot speed and the sample cooling conditions. The four experimental factors were varied as described above. The carrier gas flow rate was also adjusted to ensure that the powder particles were injected properly in the center of the plasma flame in each case. This has been verified by means of particle diagnostic tools. The coating thickness was

Table 2 Coating runs resulting from the fractional factorial experimental plan shown in Table 1

No.	Coating run	Argon	Current	Spraying distance	Disc speed	Torch power, kW	Coating temperature, °C	Coating thickness, µm
0	M-08-986-f4	Medium	Medium	Medium	Medium	39.6	180	600
1	M-08-992-f4	Low	Low	Low	Low	32.2	190	508
2	M-08-993-f4	Low	Low	High	High	32.0	120	486
3	M-08-995-f4	Low	High	Low	High	42.7	300	533
4	M-08-996-f4	Low	High	High	Low	42.8	120	523
5	M-08-997-f4	High	Low	Low	High	33.7	200	518
6	M-08-998-f4	High	Low	High	Low	33.6	120	489
7	M-08-999-f4	High	High	Low	Low	47.3	340	590
8	M-08-1000-f4	High	High	High	High	47.4	200	551
9	M-08-1001-f4	Medium	Medium	Medium	Medium	39.4	200	519

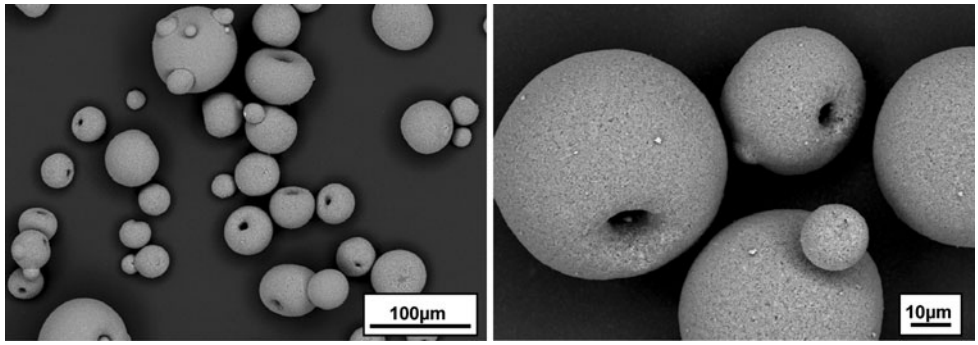

Fig. 1 Scanning electron micrographs of the spray-dried magnesia spinel powder (Jülich in-house production) used as feedstock material

Table 3 Characteristic data for the used spray-dried alumina magnesia spinel powder

Powder	AMO 278 I
Apparent density	1.34 g/cm^3
Tap density	1.58 g/cm^3
True density	3.70 g/cm^3
BET	3.00 m^2/g
Powder feed rate	4.50 g/min
Flowability (Hall flowmeter)	56.81 s
d 10	22.5 µm
d 50	47.3 µm
d 90	95.1 µm

approximately 500-550 µm (except of reference No. 0) to allow the designated analysis.

2.3 On-Line Diagnostic Tools

In the run-up to spray each sample, the particle diagnostic tool DPV-2000 (TECNAR Automation Ltd., Saint Bruno, QC, Canada) was used to measure the in-flight particle temperatures and particle velocities. The DPV-2000 is based on two-color-pyrometry and time-of-flight measurement. The measurement volume is very small (<1 mm^3) and the data is collected for individual particles. A total number of 5000 particles were measured at the centerline of the plasma jet. A more detailed description can be found in Ref 14.

2.4 Characterization Methods

In the following applied characterization methods are listed. Detailed descriptions can be found in the cited references.

- Hardness measurements were done on a Vickers hardness $HV_{0.5}$ scale (cp. Ref 15) with a test load of 4.903 N. Twenty indentations per specimen cross-section were randomly distributed over the coating thickness and statistically evaluated (Weibull analysis).
- Hardness and Young's modulus measurements were carried out by instrumented depth-sensing micro-indentation technique. Young's modulus and hardness are both determined from the loading-unloading indentation curve. The hardness can be directly related to the penetration depth, and the Young's modulus can be calculated from the unloading slope (Ref 16).
- Porosity measurements were determined by image analysis as well as by mercury porosimetry (cp. Ref 17-19). For the image analysis both SEM images (BSE mode, magnification ×500) and optical microscope images (magnification ×400) were used to identify the more suitable ones. For the mercury porosimetry the coatings were stripped in hydrochloric acid.
- Erosion tests according to the GE specification E50TF121 (cp. the description given in Ref 3) were performed. To determine the GE number 600 g of alumina particles (~50 µm) impinge on a coated surface at a 20° angle with a standoff distance of 100 mm. The deepest point of erosion is measured by a ball micrometer and the GE erosion number is calculated by dividing the test time by the erosion depth (inch ×1000). The GE number is given in s/mil and represents the time in seconds necessary to erode 25.4 µm of the coating. A higher erosion number means better erosion resistance.
- Abradability tests were carried out on the Sulzer Innotec rub-in rig (cp. Fig. 2 and the description given

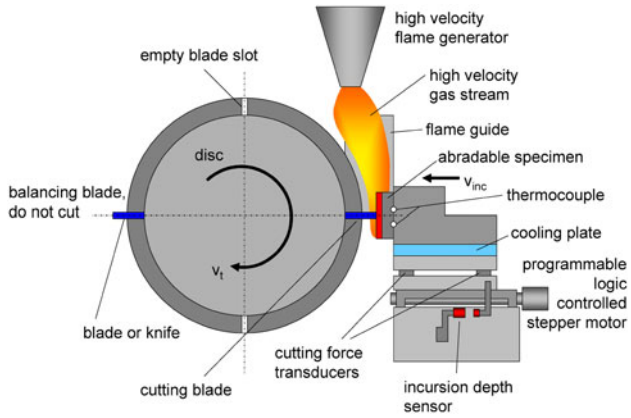

Fig. 2 Schematic drawing of the Sulzer Innotec abradability test rig (Ref 3)

in Ref 3). This rig is capable to be operated up to 1200 °C. The standard rotor can be fitted with different blade tip types. The blade tip speed can be adjusted from 30 to 410 m/s and the incursion rate from 2 to 2000 μm/s. In this investigation, the test temperatures were 800, 1000, and 1200 °C. The blade tip speed was 410 m/s and the incursion rate 50 μm/s.

3. Results and Discussion

The values of Vickers hardness ($HV_{0.5}$) and porosity are given in Table 4 for all DoE samples. From this, the three spraying parameters for a ''soft'', ''medium'' and ''hard'' Mg spinel coating were identified (italicized in Table 4). The ''medium'' one was the standard parameter setup, with a Vickers hardness of approximately 600 $HV_{0.5}$. The setup of sample No. 5 was used as ''soft'' condition showing a hardness value of about 400 $HV_{0.5}$, and as ''hard'' condition the sample setup No. 3 with approximately 800 $HV_{0.5}$. These three types of coatings were used to coat incursion test samples (test results will be presented in the following).

In Fig. 3, micrographs of the DoE and reference samples are presented, corresponding to the magnesia spinel coatings denoted as ''soft'' (No. 5), ''medium'' (No. 9) and ''hard'' (No. 3). The porosity determined by optical microscopy and image analysis is also given (Fig. 3). The different microstructures and the clearly higher amount of pores, overspray (fine-grained particle clusters) and unmolten particles for the specimen No. 5 is obvious. The most dense coating was achieved with the setup No. 3 (''hard'').

A comparison between the different measured porosity values shows that the values resulting from image analysis are lower than the ones determined by mercury porosimetry. This effect has been found before because small pores can often not be resolved with this kind of analysis technique. The porosity determined with SEM images is slightly higher than the one determined by optical microscopy presumably due to the better resolution of the SEM micrographs. But a good correlation prevails with a coefficient of determination $r^2 = 0.82$.

A correlation of hardness and porosity was found as shown in Fig. 4, where the measured $HV_{0.5}$ values are plotted against the porosity determined by optical microscopy and image analysis. An increase in porosity with decreasing hardness can be seen. A linear fit for the data is quite good with a coefficient of determination $r^2 = 0.90$.

The results of the hardness measurements by microindentation technique are shown in Fig. 5. The measurements were carried out at three different test loads (10, 100 and 1000 mN). The low and the high hardness values are confirmed for run 997 (parameter No. 5, ''soft'') and run 995 (parameter No. 3, ''hard''), respectively.

The results presented above were analyzed with the software Statistica7 (StatSoft (Europe) GmbH, Hamburg, Germany). To identify the significant parameters, especially for the hardness and the porosity, some Pareto charts of the standardized effect estimates were plotted. Beside the hardness also the deposition efficiency was included as target value to consider the cost-effectiveness of the process. The variation of the powder feed rate was found to have no significant influence on the interesting coating properties, so this parameter was ignored.

Figure 6 shows the standardized effect estimates on the target values hardness and deposition efficiency. In both cases, the argon flow rate has the main influence, followed by the current. For the deposition efficiency the argon flow rate is much more significant than for the hardness. In both cases it has the same tendency. Thus, the argon flow rate has to be reduced and the current has to be increased to increase the hardness of the coating or the deposition efficiency. Hence, a suitable setup for abradable coatings is difficult to find because an increased deposition efficiency and a decreased hardness are desired but not attainable at the same time.

Significant parameters for the porosity (in this case the values from mercury porosimetry were used) and the Young's modulus could not be detected, because the level of significance of 95% was not reached for any parameter. The interdependence between process parameters and particle characteristics (measured by DPV-2000) as an intermediate condition and subsequently between particle characteristics and microstructural characteristics was also investigated. Within the investigated range of parameter

Table 4 Results of hardness and porosity measurements

No.	Coating run	Hardness Weibull $HV_{0.5}$	Hardness Weibull r^2	Hardness Weibull shape factor	Porosity LiMi mean, %	Porosity LiMi sd, %	Porosity SEM/BSE mean, %	Porosity SEM/BSE sd, %	Porosity Hg, %	Deposition efficiency, %
0	M-08-986-f4	571	0.96	4.82	12.52	1.32	15.34	1.16	20.52	58.9
1	M-08-992-f4	658	0.98	3.97	9.27	1.18	12.56	0.60	15.08	72.6
2	M-08-993-f4	694	0.96	7.33	9.88	0.84	11.20	0.49	16.93	63.2
3	*M-08-995-f4*	*816*	0.98	3.32	7.74	0.88	10.12	0.32	11.30	82.2
4	M-08-996-f4	696	0.91	11.19	10.43	0.90	10.23	0.81	18.24	68.9
5	*M-08-997-f4*	*391*	0.97	5.03	22.62	2.73	22.69	0.92	22.98	24.0
6	M-08-998-f4	433	0.83	5.79	19.61	1.08	16.31	0.50	20.83	22.1
7	M-08-999-f4	737	0.93	4.81	13.48	2.55	17.23	1.14	19.73	58.5
8	M-08-1000-f4	572	0.88	4.88	13.85	1.14	16.16	0.53	19.55	46.3
9	*M-08-1001-f4*	*604*	0.98	3.87	15.72	1.33	15.18	0.46	20.71	59.8

Note: The values in italics indicate the spraying parameters used for coating the incursion test plates

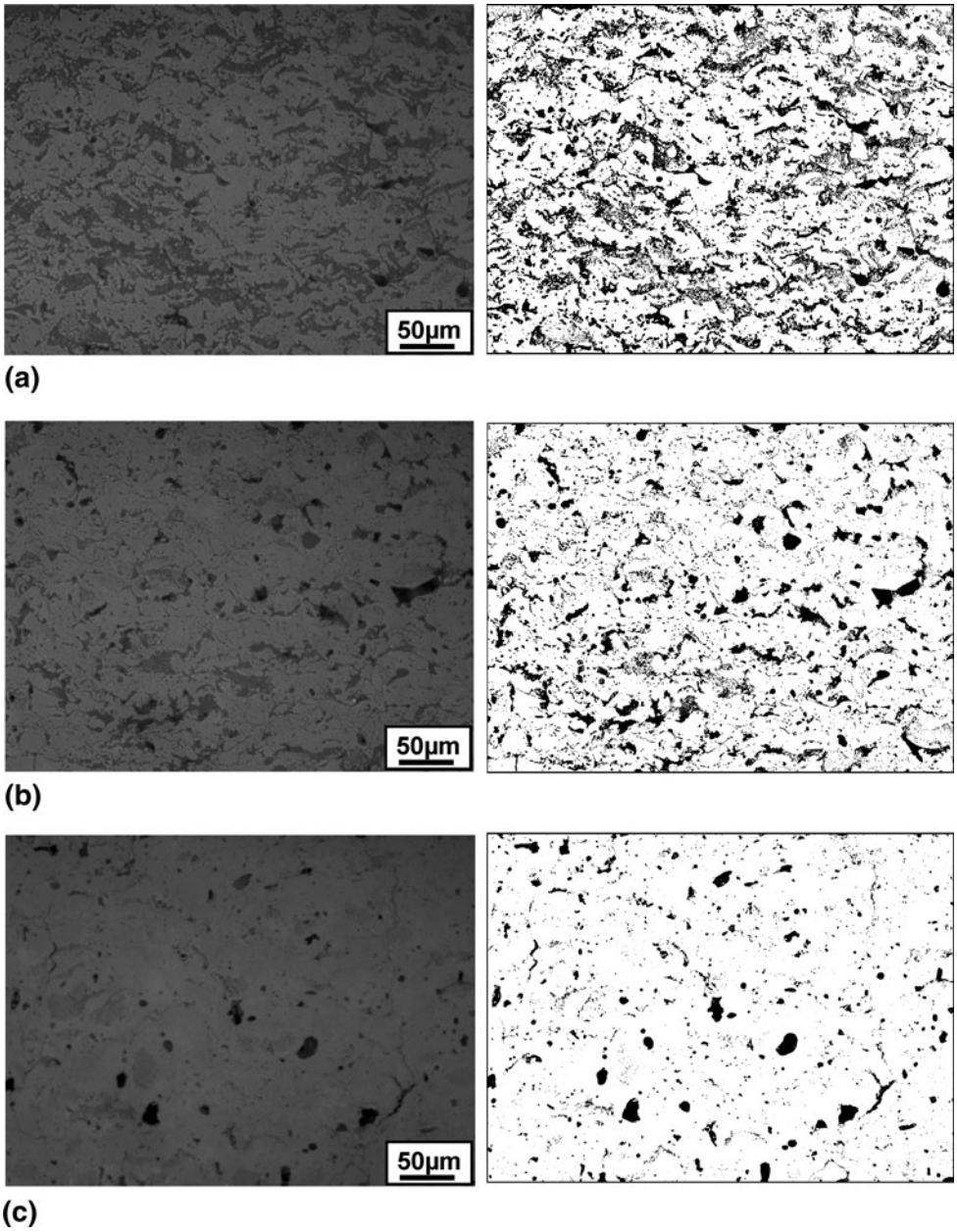

Fig. 3 Microstructure and porosity analysis for the DoE samples (a) No. 5 (soft), (b) No. 9 (medium) and (c) No. 3 (hard)

settings no significance was detectable for the measured particle temperature. Nevertheless, a qualitative analysis shows that the spraying distance has to be reduced while the current has to be increased to achieve higher particle temperatures. For the particle velocity the argon flow rate was found to be significant. To increase the particle velocity, in particular the argon flow rate has to be increased. It can also be qualitatively concluded that a reduction in the spraying distance combined with an increase in current gives higher particle velocities.

Figure 7 shows a process map in which the particle temperature is plotted against the particle velocity for the eight DoE-setups and the two reference cases. Also, some contour lines are plotted for the target values hardness and porosity. They are determined based on a linear multiple regression model. Because of the simplicity of this model the standard errors for hardness and porosity are 115 $HV_{0.5}$ and 1.4%, respectively, which should be taken into account for quantitative conclusions. However, qualitative statements can be derived with good reliability.

It can be concluded that with higher particle temperature the porosity decreases and the hardness increases. Most of the particles are in a molten condition, and thus deposition of the particles is quite effective and between the splats only few voids are generated.

However, with higher particle velocity the porosity of the coating is increased and the hardness reduced. An explanation is that the dwell time of the particles in the plasma jet is shorter, which leads to a higher amount of unmolten particles. They degrade the efficiency of the deposition process (less lamellar deposited splats). Furthermore, the molten particles are more fragmentized at impact on the substrate due to higher velocities. Hence, rough splat rims and subdroplets are formed.

Both effects of increased particle velocities, the higher amount of unmolten particles as well as the fragmentation of the molten particles lead to more fine voids within the coating. There may be also some kind of bouncing-off effect, which may also contribute to higher porosity and softer coatings.

The linear regression model was used also to determine optimum process parameter sets according to desired hardness and deposition efficiency values. A small argon flow rate, a high current as well as a small spraying distance should be used to achieve a high coating hardness and also a good deposition efficiency. For this ''hard'' setup the predicted deposition efficiency of 77.6% and hardness of 820 $HV_{0.5}$ were in good agreement with the measured values of run No. 3 (deposition efficiency 82.2% and hardness 816 $HV_{0.5}$, respectively, cp. Table 4).

Because a correlation is given for coating properties and particle properties, the diagnostic tool DPV-2000 was also used during plasma spraying of magnesia spinel abradables on batches of turbine components (cp. Fig. 8). Particle properties in a defined range should keep the coating properties also in the desired range. Low scatter of the recorded particle characteristics and coating

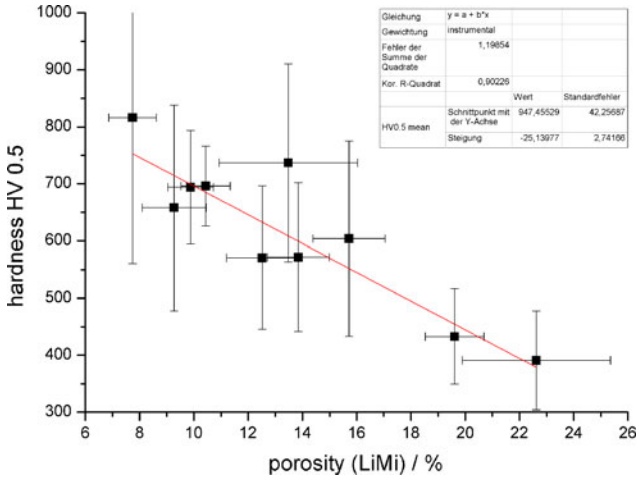

Fig. 4 Correlation between Vickers hardness $HV_{0.5}$ and porosity (determined by optical microscopy and image analysis)

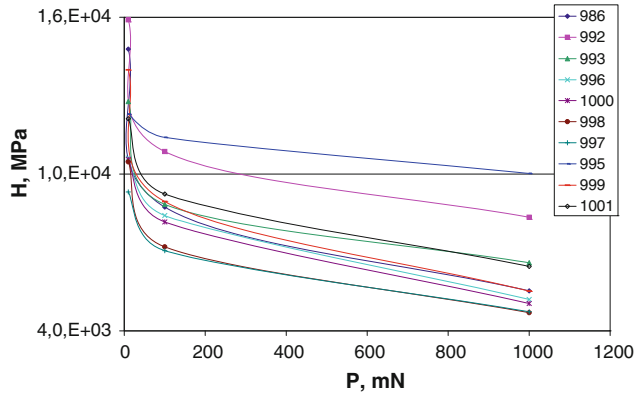

Fig. 5 Hardness measured by microindentation technique at three different test loads (10, 100 and 1000 mN)

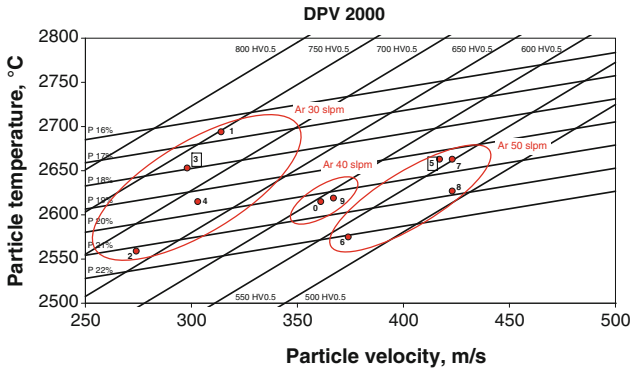

Fig. 7 Process map with particle characteristics and contour lines for target values hardness and porosity

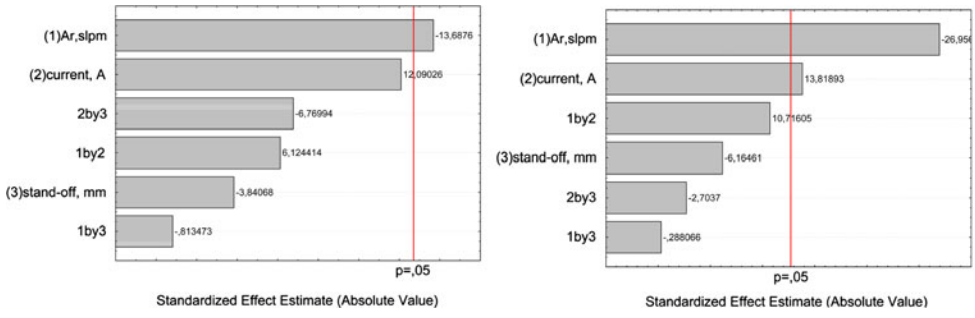

Fig. 6 Pareto charts of standardized effect estimates for hardness (test load 4.903 N, left) and deposition efficiency (right)

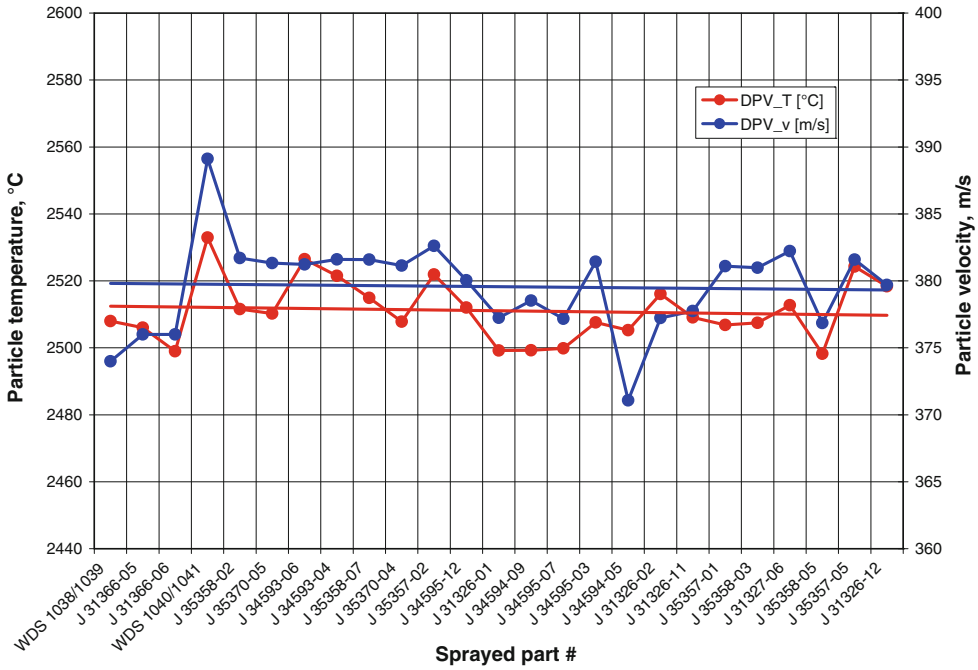

Fig. 8 Process monitoring by DPV-2000 during spraying of batches of turbine components

Table 5 Results of the GE erosion tests

No.	Coating run	GE erosion number Normal E, s/mil
1	M-08-992-f4	6.87
2	M-08-993-f4	5.08
3	*M-08-995-f4*	*15.58*
4	M-08-996-f4	7.42
5	*M-08-997-f4*	*1.64*
6	M-08-998-f4	2.02
7	M-08-999-f4	4.73
8	M-08-1000-f4	4.00
9	M-08-1001-f4	5.52

properties showed a good reproducibility of the spraying process, so that the coating properties are expected to be kept within narrow tolerances.

Table 5 shows the results of the GE erosion tests carried out for the DoE samples. The GE erosion number is calculated from the deepest point of erosion and the test time. For the hard setup (No. 3) the highest GE number of 15.58 s/mil was achieved, which means a very good erosion resistance. For the soft setup the GE number was only 1.64 s/mil. This result shows also a good correlation with the hardness measurements mentioned before. A commonly acceptable GE erosion number for abradable ceramic coatings (mostly determined for the standard material YSZ) is in the range from 2 to 5 s/mil. The reference sample (No. 9, ''medium'') shows a GE number of 5.52 s/mil, which is obviously at the upper limit.

This was confirmed by the incursion tests which were carried out for samples sprayed with the soft, medium and hard spraying parameters (cp. Fig. 9). A part of the ''medium'' samples showing approximately 600 $HV_{0.5}$ shows a good cut-in behavior with low blade wear. But some of them did not cut very well and produced a higher blade wear. Only for the soft coatings (approximately 400 $HV_{0.5}$) the abradability seems to be thoroughly good and independent of the applied test temperature.

4. Conclusion

The DoE work gives a good overview on the significant process parameters and the suitable characterization methods for abradable coatings. The hardness can be used as an indication for the abradability. It should be in the range of 500 $HV_{0.5}$. A hardness of approximately 600 $HV_{0.5}$ seems to be the upper end at which a good cut-in is no longer reliably reproducible. The GE erosion number is also a good indication (and simpler to perform than an incursion test). With a value of approximately 5.5 s/mil the allowable limit according to a good cut-in performance seems to be reached.

Furthermore, the following conclusions can be made from the statistical evaluation of the DoE.

- In general, the spraying parameter with the largest significant effect is the argon flow rate which mainly affects the particle velocity.
- To change the hardness of a magnesia spinel coating both the particle velocity and the particle temperature are influencing factors.
- To change the porosity of a magnesia spinel coating the particle temperature is the main influencing factor.

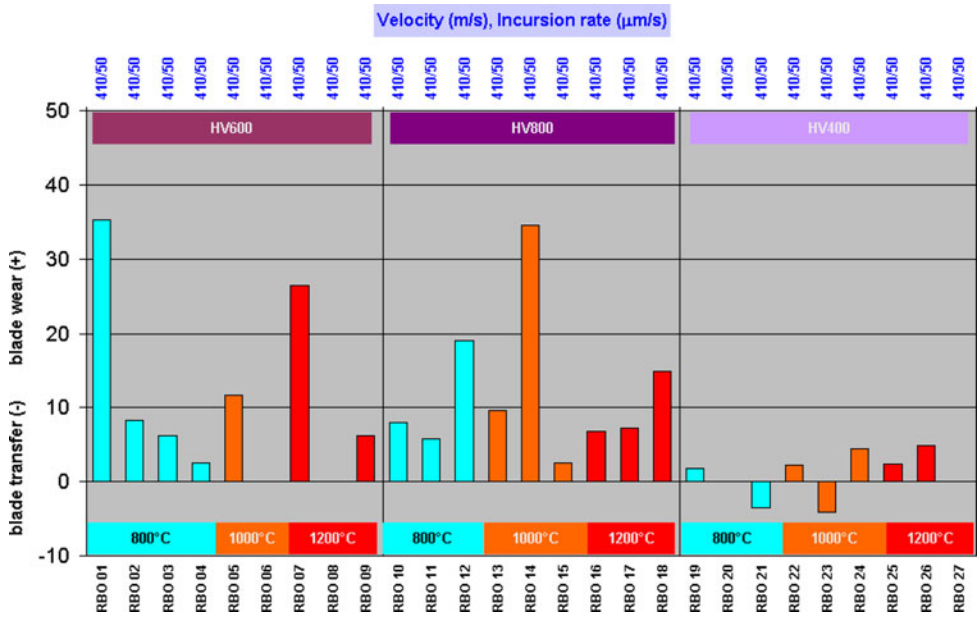

Fig. 9 Incursion test results for samples with different coating hardness (the blade wear is given as a percentage of the total incursion depth)

- Hardness and porosity show a similar dependence on particle temperature and velocity, which confirms the correlation between these values (cp. Fig. 4).
- To increase the particle velocity in particular, the argon flow rate has to be increased. Also, a reduction in the spraying distance as well as an increase of the current gave higher particle velocities, but these effects do not reach the significance level.
- For the particle temperature no significant effects were detectable within the investigated ranges of parameters. A trend shows increasing temperatures with decreasing spraying distance and increasing current.

Acknowledgments

The authors gratefully acknowledge the support of Dr. Jürgen Malzbender (Forschungszentrum Jülich GmbH, IEF-2) who carried out the hardness and Young's modulus measurements with instrumented microindentation technique. Mr. Mark Kappertz (IEF-1) kindly prepared the cross-sections of the samples and Dr. Doris Sebold (IEF-1) did the SEM work.

References

1. R.K. Schmid, F. Ghasripoor, M. Dorfman, and X. Wei, An Overview of Compressor Abradables, *Thermal Spray: Surface Engineering via Applied Research*, C.C. Berndt, Ed., May 8-11, 2000 (Montréal, QC, Canada), ASM International, 2000, p 1087-1093
2. D. Sporer, S. Wilson, I. Giovannetti, A. Refke, and M. Giannozzi, On the Potential of Metal and Ceramic Based Abradables in Turbine Seal Applications, *Proceedings of the Thirty-Sixth Turbomachinery Symposium*, Sept 11-13, 2007 (Texas A&M University, College Station, TX), 2007, p 79-86
3. D. Sporer, M. Dorfman, L. Xie, A. Refke, I. Giovannetti, and M. Giannozzi, Processing and Properties of Advanced Ceramic Abradable Coatings, *Thermal Spray 2007: Global Coating Solutions*, M.R. Marple, M.M. Hyland, Y.-C. Lau, C.-J. Li, R.S. Lima, and G. Montavon, Ed., May 14-16, 2007 (Beijing, Japan), ASM International, 2007, p 495-500
4. R.S. Lima, B.R. Marple, A. Dadouche, W. Dmochowski, and B. Liko, Nanostructured Abradable Coatings for High Temperature Application, *Thermal Spray 2006: Building on 100 Years of Success*, M.R. Marple, M.M. Hyland, Y.-C. Lau, R.S. Lima, and J. Voyer, Ed., May 15-18, 2006 (Seattle, WA, USA), ASM International, 2006
5. R. Schmid, "New High Temperature Abradables for Gas Turbines," Ph.D. Thesis, Swiss Federal Institute of Technology Zurich, 1997
6. F. Ghasripoor, R. Schmid, and M. Dorfman, Abradable Coatings Increase Gas Turbine Efficiency, *Mater. World*, 1997, **5**(6), p 328-330
7. R. Vaßen, F. Traeger, and D. Stöver, New Thermal Barrier Coatings Based on Pyrochlore/YSZ Double-Layer Systems, *Int. J. Appl. Ceram. Technol.*, 2004, **1**(4), p 351-361
8. R. Vaßen, A. Stuke, and D. Stöver, Recent Developments in the Field of Thermal Barrier Coatings, *J. Therm. Spray Technnol.*, 2009, **18**(2), p 181-186
9. Shroud Segment for a Turbomachine, U.S. Patent US 2005/0276688 A1
10. L. Pawlowski, *The Science and Engineering of Thermal Spray Coatings*, 2. ed., Wiley, Chichester, 2008
11. A. Kulkarni, A. Vaidya, A. Goland, S. Sampath, and H. Herman, Processing Effects on Porosity-Property Correlations in Plasma Sprayed Yttria-Stabilized Zirconia Coatings, *Mater. Sci. Eng. A*, 2003, **A359**(1-2), p 100-111
12. M. Friis and C. Persson, Process Window for Plasma Spray Processes, *Thermal Spray 2001: New Surfaces for a New Millennium*, C.C. Berndt, K.A. Khor, and E.F. Lugscheider, Ed., May 28-30, 2001 (Singapore), ASM International, 2001, p 1313-1319
13. C. Pierlot, L. Pawlowski, M. Bigan, and P. Chagnon, Design of Experiments in Thermal Spraying: A Review, *Surf. Coat. Technol.*, 2008, **202**(18), p 4483-4490

14. G. Mauer, R. Vaßen, and D. Stöver, Comparison and Applications of DPV-2000 and Accuraspray-g3 Diagnostic Systems, *J. Therm. Spray Technol.*, 2007, **16**(3), p 414-424
15. Advanced Technical Ceramics—Mechanical Properties of Monolithic Ceramics at Room Temperature—Part 4: Vickers, Knoop and Rockwell Superficial Hardness; German Version EN 843-4:2005, DIN Deutsches Institute für Normung e.V., p 1-22
16. J. Malzbender and R.W. Steinbrech, Determination of the Stress-Dependent Stiffness of Plasma-Sprayed Thermal Barrier Coatings Using Depth-Sensitive Indentation, *J. Mater. Res.*, 2003, **18**(8), p 1975-1984
17. G. Bertrand, P. Bertrand, P. Roy, C. Rio, and R. Mevrel, Low Conductivity Plasma Sprayed Thermal Barrier Coating Using Hollow PSZ Spheres: Correlation Between Thermophysical Properties and Microstructure, *Surf. Coat. Technol.*, 2008, **202**(10), p 1994-2001
18. J. Matějíček, B. Kolman, J. Dubský, K. Neufuss, N. Hopkins, and J. Zwick, Alternative Methods for Determination of Composition and Porosity in Abradable Materials, *Mater. Charact.*, 2006, **57**(1), p 17-29
19. J. Ilavsky, C.C. Berndt, and J. Karthikeyan, Mercury Intrusion Porosimetry of Plasma-Sprayed Ceramic, *J. Mater. Sci.*, 1997, **32**(15), p 3925-3932